

REPORT ITU-R P.2097

Transionospheric radio propagation**The Global Ionospheric Scintillation Model (GISM)**

(2007)

TABLE OF CONTENTS

	<i>Page</i>
1 Introduction	2
2 Inhomogeneities characteristics.....	2
3 Dependency of inhomogeneities on the latitude.....	3
4 GISM propagation model	5
4.1 Medium modelling.....	5
4.2 Algorithm.....	5
5 Scintillations at receiver level	7
5.1 GPS receiver architecture	7
5.2 Phase noise at receiver level.....	8
6 Loss of lock probability.....	11
7 Positioning errors.....	13
8 Simultaneous loss of lock.....	15
9 Comparisons models results and measurements	16
10 References	18

1 Introduction

Ionospheric scintillations are rapid variations of phase and amplitude of a signal, which passes through the ionosphere. They are very pronounced in equatorial regions where they appear every day after sunset and may last for a few hours. They are related in particular to solar activity and the season. The main factors whose dependency has been established are indicated hereafter. At mid-latitudes, the scintillations are rather weak, except during conditions of ionospheric storms. Very strong effects relating to storms can be observed in the auroral regions.

Scintillations are created by random fluctuations of the medium's refractive index, which are caused by inhomogeneities inside the medium. These inhomogeneities in the ionosphere are the result of several mechanisms ($E \times B$ gradient drift, streaming instabilities (Kelvin Helmholtz), Rayleigh Taylor, etc.). Characteristic dimensions and different growth rates correspond to each one of the existing processes. The overall problem is very complex and difficult to reproduce theoretically on a large scale.

The inhomogeneities create a number of modifications of transmitted signals, among them phase and intensity fluctuations, fluctuations of the angle of arrival, dispersivity, Doppler, etc. This problem has been studied extensively in the past. Methods presented include the Rytov approximation in the case of weak fluctuations, the phase screen theory and the parabolic equation (PE) method. The Global Ionospheric Scintillation Model (GISM) uses the multiple phase screen (MPS) technique. It consists in a resolution of the PE for a medium divided into successive layers, each of them acting as a phase screen.

The GISM model provides the statistical characteristics of the transmitted signals, in particular the scintillation index, fade durations and the cumulative probability of the signal allowing the determination of the margins to be included in a budget link. Maps of the scintillation index S4 and of the phase standard deviation may also be obtained.

2 Inhomogeneities characteristics

Ionosphere inhomogeneities are of two kinds: random inhomogeneities and travelling ionospheric disturbances (TID). These last have large dimensions and are equivalent to gravity waves. They are beyond the scope of GISM. Only the random inhomogeneities are taken into account by the model. The following parameters have to be specified:

- the spectral density of their electron density fluctuations;
- their correlation distance;
- the altitude to which they develop;
- their velocity and direction of displacement.

a) Spectral density

The scintillations spectrum usually exhibits a linear variation with the logarithm of frequency. The most important parameter is the inclination index of this spectrum: p . The cut-off frequency is related to the correlation distance of inhomogeneities.

The value of p depends on the specific conditions of development of the turbulences, in particular the instability process involved, the latitude, the altitude, etc. As observed by measurements, in particular with satellite ETS-2 [Afraimovitch *et al.*, 1994], the slope value is usually between -2 and -4 .

b) *Correlation length*

The correlation length is of primary importance in the characterization of the inhomogeneities. With respect to these inhomogeneities, the medium may be simulated by a number of scatterers randomly distributed in space. One important parameter to consider is the size of the first Fresnel zone at the altitude under examination. As an example, for a transmitted signal at frequency 137 MHz and at height 300 km, the size of the first Fresnel zone is $r = \sqrt{\lambda h} \approx 1$ km. Inhomogeneities whose size is lower or comparable to this dimension will create scintillation phenomena.

As for the power spectrum index value, the coherence length of inhomogeneities varies with local specific conditions. To perform a propagation calculation, the medium is considered as statistically homogeneous. To do this, we assign to each particular region of the ionosphere (altitude, latitude) typical characteristics of the inhomogeneities at the region under examination. The mean value of the correlation length deduced from measurements is about 800 m at the *F* layer altitude [Afraimovitch *et al.*, 1994].

Drift of the irregularities causes a Doppler shift of the diffraction pattern. Both the direction and the modulus of velocity are important and are taken into account in the characterization of the statistical properties of the medium.

c) *Height of irregularities*

The height at which the instabilities develop may be obtained from the diffraction pattern of the transmitted signals. This last is related to the location of the first Fresnel zone. The corresponding frequency is obtained from the spectral density spectrum of the irregularities. Once this frequency is measured, the altitude where the irregularities develop can be easily obtained. Histograms of measurements show a peak value at altitudes between 300 and 500 km, consequently at the *F* layer altitude [Afraimovitch *et al.*, 1994 and Mc Dougall, 1981].

3 Dependency of inhomogeneities on the latitude

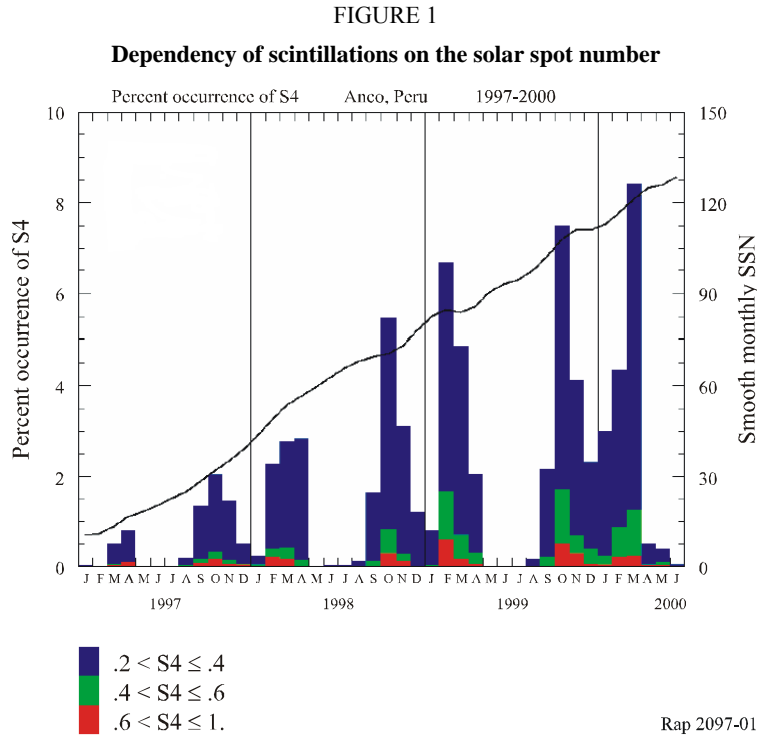
Scintillations are most severe and prevalent in and north of the auroral zone and near the geomagnetic equator [Aarons, 1982]. The equatorial region extends approximately from -20° to 20° and auroral regions from 55° to 90° . These boundaries change with the time of the day, the season of the year, the sunspot number and the magnetic activity.

a) *Equatorial scintillations*

Scintillation is predominantly a night time phenomenon in the equatorial region occurring for more than 40% of the year during the 20:00-02:00 local time period. It also shows a strong seasonal dependence with a pronounced minimum at the southern solstice and relatively high scintillation activity at the northern solstice. Equatorial scintillations also show a tendency to occur more often during years in which the sunspot number is high. The r.m.s. amplitude of electron density irregularities is equal to 20% in the most severe cases.

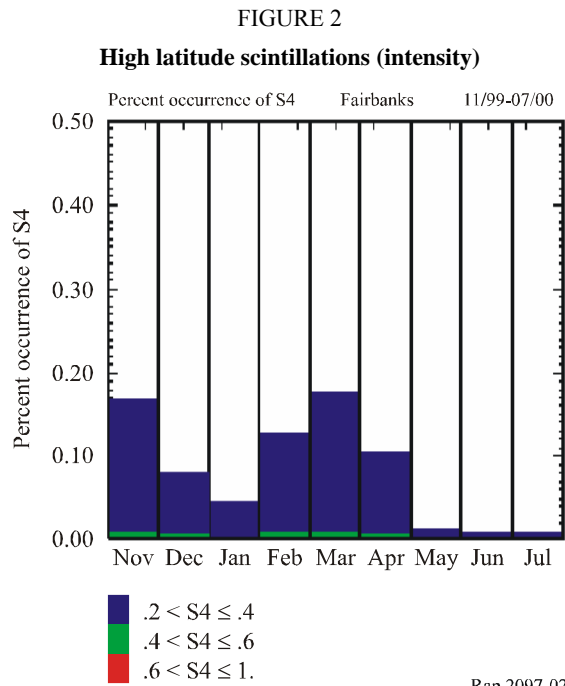
Two regimes may be identified. For values of the amplitude scintillation index (S4) below approximately 0.5, the RMS value of phase and intensity fluctuations seems to be linearly correlated and approximately equal. For greater values of S4, there is no obvious correlation and measured values are greater for intensity than for phase [Doherty *et al.*, 2000].

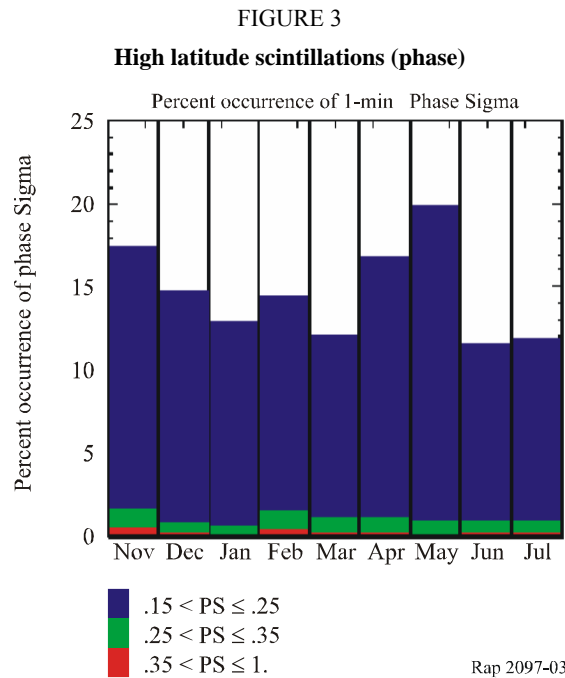
If we considered the case of GPS L2 scintillations, the typical value of S4 at equatorial regions is 0.3. Its occurrence is related to the season and the solar activity. It may reach a value of 0.5 with an occurrence 10% below and a value of 0.8 or even 1 in a few cases.



b) *High latitude scintillations*

Contrary to equatorial fluctuations, the polar fluctuations exhibit more phase than intensity fluctuations. The intensity scintillation index is usually quite low. It rarely exceeds 0.2 and the probability of occurrence is very low in summer and always below the values obtained at equatorial regions. The situation is reverse for phase fluctuations. They may exist all the year. The values are quite high and seem to be related to magnetic activity.





4 GISM propagation model

4.1 Medium modelling

The electronic density inside the medium is calculated by the NeQuick model developed by the University of Graz and ICTP Trieste. Inputs of this model are the solar flux number, the year, the day of the year and the local time. It provides the electronic density average value for any point in the ionosphere (latitude, longitude, altitude). The NeQuick model is used as a subroutine in the GISM model.

Fluctuations of the electronic density mostly develop at night-time, at the F layer altitude and at equatorial and polar latitudes. To account for these fluctuations in the model, a database has been constituted from results published in the literature.

The magnetic parameters are computed from a Schmidt quasi-normalized spherical harmonic model of the magnetic field. These are the declination, the inclination, the vertical intensity and the components of the field. Accuracies for the angular components (declination and inclination) are less than 30 min. Accuracies for the force components (horizontal, north, east, vertical and total force) are generally less than 25 nanoTeslas. The code used has been developed by the National Geophysical Data Center, NOAA, Boulder, Colorado. It is used as a subroutine in the GISM code. Given the location of a point on a ray, it provides the magnetic parameters. This allows the calculation of the Faraday rotation.

4.2 Algorithm

There are two kinds of propagation errors:

- mean errors;
- scintillations and more generally higher order moments of the signal.

Mean errors are obtained solving the ray equation. The ray differential equation is solved by the Runge Kutta algorithm. The line of sight (LoS) is defined taking the electron density gradient at each point along the ray into account. This is done with respect to the three axes in a geodesic referential system. This is an iterative algorithm. It is stopped when the ray crosses the plane perpendicular to the line of sight and containing the source point. The mean errors: range, angular and Faraday rotation are subsequently determined.

The calculation of fluctuations is a 2D calculation. The first dimension is the LoS previously determined. The second dimension is perpendicular to that one. Symmetry of revolution is consequently assumed. To obtain the signal scintillations, the propagation equation is solved considering that the dielectric constant, ϵ , and subsequently the wave number k , are random numbers.

$$\nabla^2 U + k^2 U = 0 \quad (1)$$

Assuming that the field variation is mainly in the direction perpendicular to the main propagation axis (parabolic approximation), equation (1) can be written as:

$$2jk \frac{\partial \langle U \rangle}{\partial z} + \nabla_t^2 \langle U \rangle + k^2 \langle \epsilon U \rangle = 0 \quad (2)$$

where ∂z is the variable related to the main propagation axis.

To solve equation (2), the medium is divided into successive layers, each one being characterized by stationary statistical properties. Iterating successively scattering and propagation calculations gives the solution as detailed below.

In the Fourier transform domain, equation (2) can be written:

$$2jk \frac{\partial \langle U \rangle}{\partial z} - p^2 \langle U \rangle + k^2 \langle \epsilon U \rangle = 0 \quad (3)$$

Variables p and x are the corresponding variables in the Fourier transform:

$$U(z, p) = \int U(x, z) \exp(-jpx) dx \quad (4)$$

The x variable is the variable related to the direction perpendicular to the propagation main axis (the z axis). The solution is consequently obtained in the (x, z) plane.

The equation (3) solution is:

$$U(x, z + \delta z) = \int U(z + \delta z, p) \exp(jpz + jp^2 \delta z / (2k)) dp \quad (5)$$

This equation is the Kirchhoff integral equation. It can be used to calculate the field radiated by an arbitrary field distribution on a screen. It applies in particular to the free-space far-field calculation from the ionized medium output to the observation point.

The calculation proceeds by alternating integral calculations of equations (4) and (5). All these calculations are performed using fast Fourier transform (FFT) techniques. This technique is referred in the literature as multiple phase screen (MPS) technique.

Random medium synthesis

The spectral density of the phase at the output of the medium is written as the product of the Fourier transform of a centred Gaussian random variable and the square root of the spectral density of the signal to be synthesized. The resulting random variable meets the required conditions. The corresponding signal is obtained taking the inverse Fourier transform of this product.

For a given layer the transmitted phase spectral density of the signal is:

$$\gamma_{\Phi}(q) = \frac{C_p}{(q_0^2 + q^2)^{P/2}} \quad (6)$$

with:

$$q_0 = 2\pi/L_0$$

L_0 : average size of the inhomogeneities (m).

Input data are the slope of the electron density spectrum, the dimension of inhomogeneities and their drift velocity.

FFT limitations

The extent of the medium in the direction perpendicular to the main propagation axis must be large compared to the autocorrelation distance of the inhomogeneities.

Moreover, the space step must be a fraction of a wavelength.

These two requirements influence the number of points used in the FFT algorithm. It has been set to 16 384 for signal propagation up to 2 GHz. It should be increased for propagation at higher frequencies.

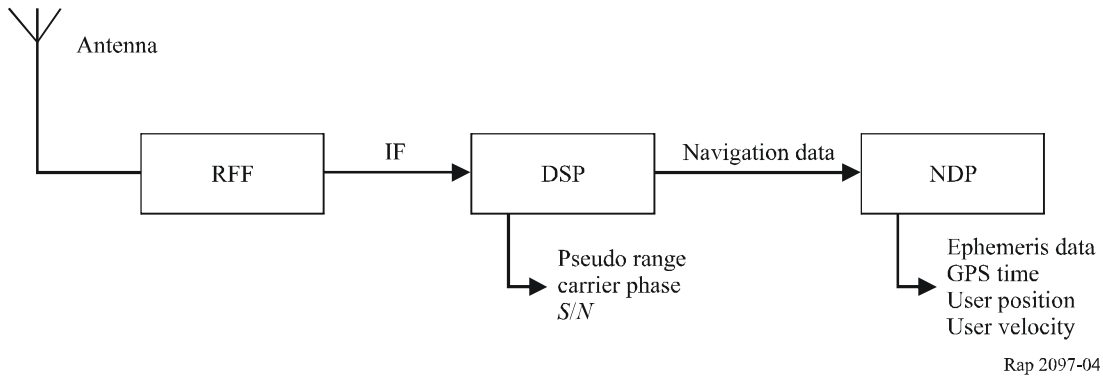
5 Scintillations at receiver level**5.1 GPS receiver architecture**

A GPS receiver is a spread spectrum receiver, requiring several essential parts for acquisition, tracking and extracting useful information from the incoming satellite signal. It can be broadly divided into three sections: the RF front-end (RFF), digital signal processing (DSP) and the navigation data processing (NDP). The RFF and DSP sections generally consist of various hardware modules, whereas the NDP section is implemented using software. Figure 4 shows a simple block diagram of a typical single frequency GPS receiver with major interfaces and input/output signals of the essential blocks.

The DSP performs the acquisition and tracking of the GPS signal. Traditional signal demodulation such as those used for FM or AM cannot be used for spread spectrum signals such as GPS because the signal level is below the noise level. Instead, the signal must be coherently integrated over time so that the noise is averaged out, thereby raising the signal above the noise floor.

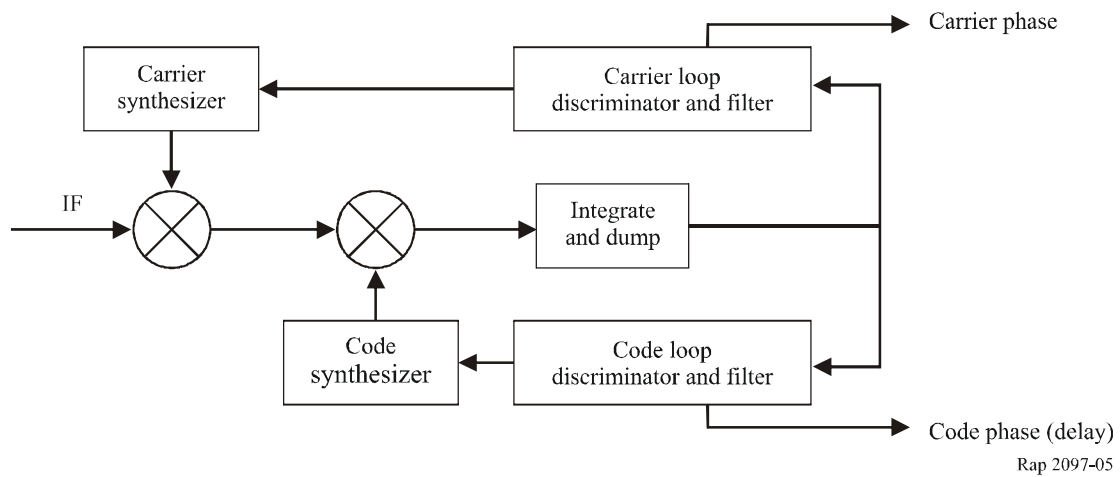
Any GPS receiver locking up on a GPS satellite has to do a two-dimensional search for the signal. The first dimension is time. The GPS signal structure for each satellite consists of a 1 023 bit long pseudo-random number (PRN) sequence sent at a rate of 1 023 Mbit/s, i.e. the code repeats every millisecond. To acquire in this dimension, the receiver needs to set an internal clock to the correct one of the 1 023 possible time slots by trying all possible values. Once the correct delay is found, it is tracked with a delay lock loop (DLL).

FIGURE 4
Block diagram of a generic GPS receiver



The second dimension is frequency. The receiver must correct for inaccuracies in the apparent Doppler frequency. Once the carrier frequency is evaluated, it is tracked with a phase lock loop (PLL). Figure 5 shows an extremely simplified PLL/DLL architecture. A more precise description of the GPS signal processing can be found in Ward [1996].

FIGURE 5
Simplified GPS digital receiver channel



5.2 Phase noise at receiver level

When the receiver is unable to track the carrier phase, the signal is lost. Loss of lock is directly related with PLL cycle slips. To evaluate the occurrence of cycle slips, the tracking error variance at the output of the PLL has to be considered. Following [Conker *et al.*, 2003] this variance is expressed as a sum of three terms:

$$\sigma_{\Phi}^2 = \sigma_{\Phi S}^2 + \sigma_{\Phi T}^2 + \sigma_{\Phi,osc}^2 \quad (7)$$

where:

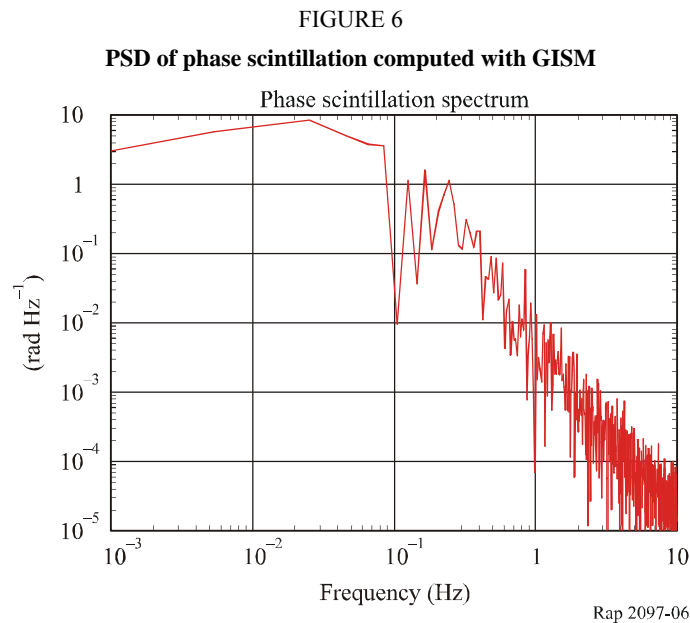
- $\sigma_{\Phi S}$: phase scintillation
- $\sigma_{\Phi T}$: thermal noise
- $\sigma_{\Phi,osc}$: receiver oscillator noise (0.122 rad) [Conker *et al.*, 2003].

The phase variance scintillation at the output of the PLL is given by [Béniguel, 2002]:

$$\sigma_{\Phi_S}^2 = \int_{-\infty}^{\infty} |1 - H(f)|^2 S_{\Phi}(f) df \quad (8)$$

where $S_{\Phi}(f)$ is the power spectral density (PSD) of phase scintillation. Figure 6 shows a phase scintillation spectrum obtained with GISM. $|1 - H(f)|^2$ is the closed loop transfer function of the PLL and depends on k , the loop order, and f_n , the loop natural frequency. Its expression is given by equation (9). Typical values are $k = 3$ and $f_n = 1.91$ Hz.

$$|1 - H(f)|^2 = \frac{f^{2k}}{f^{2k} + f_n^{2k}} \quad (9)$$



When there is no scintillation, the standard thermal noise tracking error for the PLL is:

$$\sigma_{\Phi_T}^2 = \frac{B_n}{(c/n_0)} \left[1 + \frac{1}{2\eta(c/n_0)} \right] \quad (10)$$

where:

c/n_0 : S/N

B_n : receiver bandwidth

η : predetection time.

For airborne GPS receivers, $B_n = 10$ Hz and $\eta = 10$ ms.

Amplitude scintillation alters the S/N and increases the thermal noise tracking error. According to [Aarons, 1982], in the presence of scintillation characterized by S4 index, thermal noise tracking error is given by:

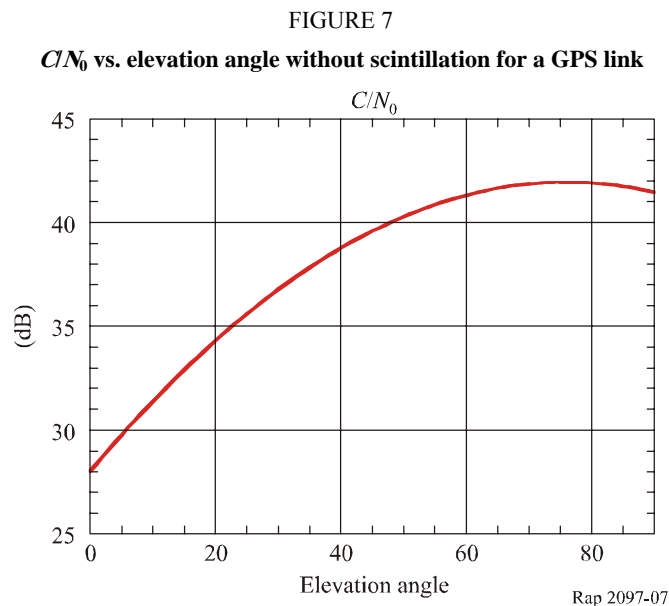
$$\sigma_{\Phi_T}^2 = \frac{B_n \left[1 + \frac{1}{2\eta(c/n_0)(1-2s_4^2)} \right]}{(c/n_0)(1-2s_4^2)} \quad (11)$$

Equation (11) needs the evaluation of the S/N .

The GPS link budget can be expressed in dB as following:

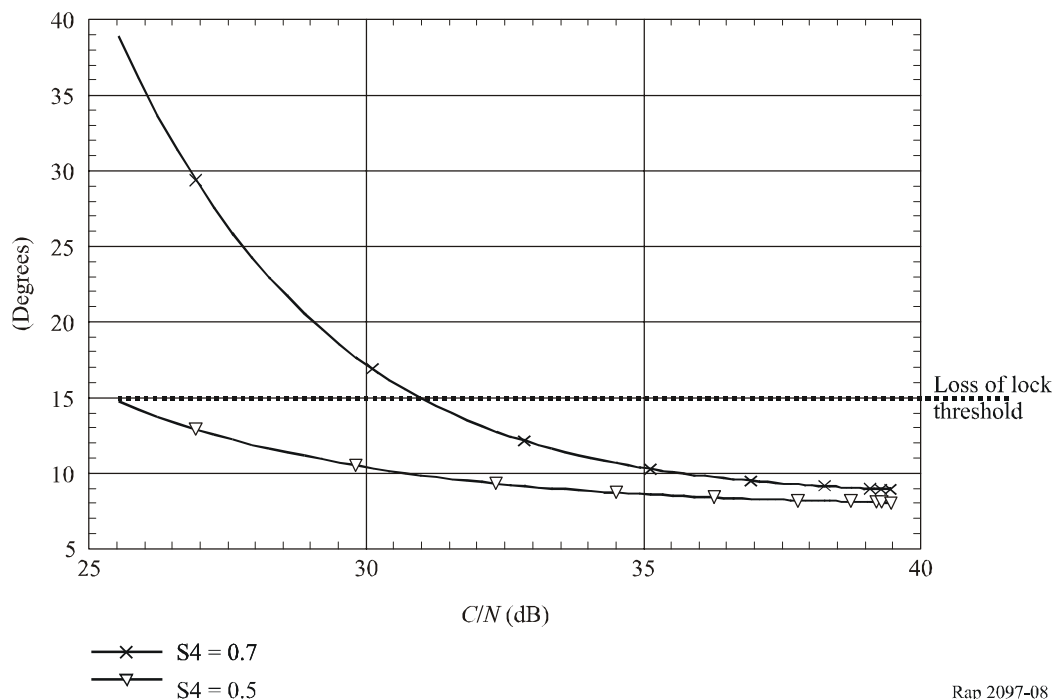
$$C/N_0 = P_0 + G_t + G_r - \text{Propagation losses} - \text{Insertion Losses} - N_0 \quad (12)$$

where P_0 is the transmitted power, G_t and G_r are antenna gains of the transmitter and the receiver antenna, respectively, and N_0 is the receiver noise density. Therefore, the S/N appears to be depending on the elevation angle as shown in Fig. 7.



Equations (11) and (8) can be used with (7) to compute the PLL tracking error variance. Figure 8 is a comparison of this variance vs. C/N_0 for $S4 = 0.7$ and $S4 = 0.5$. Loss of lock is highly probable for values above the 15° threshold. Therefore a receiver is able to tolerate scintillation if the C/N_0 is above a minimum value. This minimum is 26 dB for $S4 = 0.5$ and 32 dB for $S4 = 0.7$.

FIGURE 8
PLL standard deviation vs. C/N_0

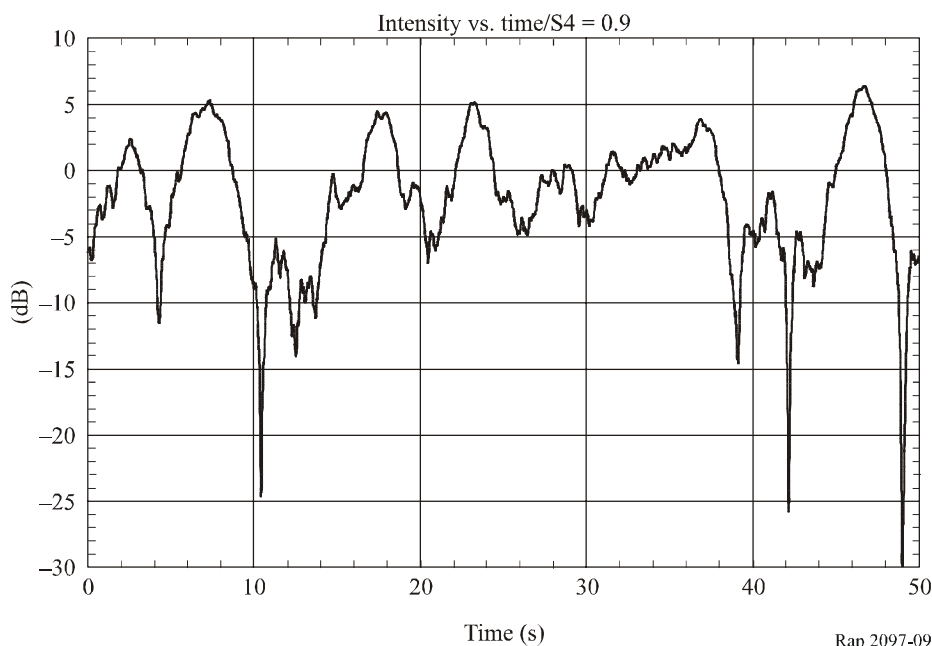


Rap 2097-08

6 Loss of lock probability

Thermal noise appears to be the essential contribution to PLL tracking error. It is the unique S_4 dependent term in (7) and the influence of S_4 is obvious in Fig. 8. A study of amplitude scintillations is detailed in Ward [1996] and leads to (11). A different approach is given below of amplitude scintillation effects on thermal noise.

FIGURE 9
Scintillation intensity vs. time computed with GISM



Rap 2097-09

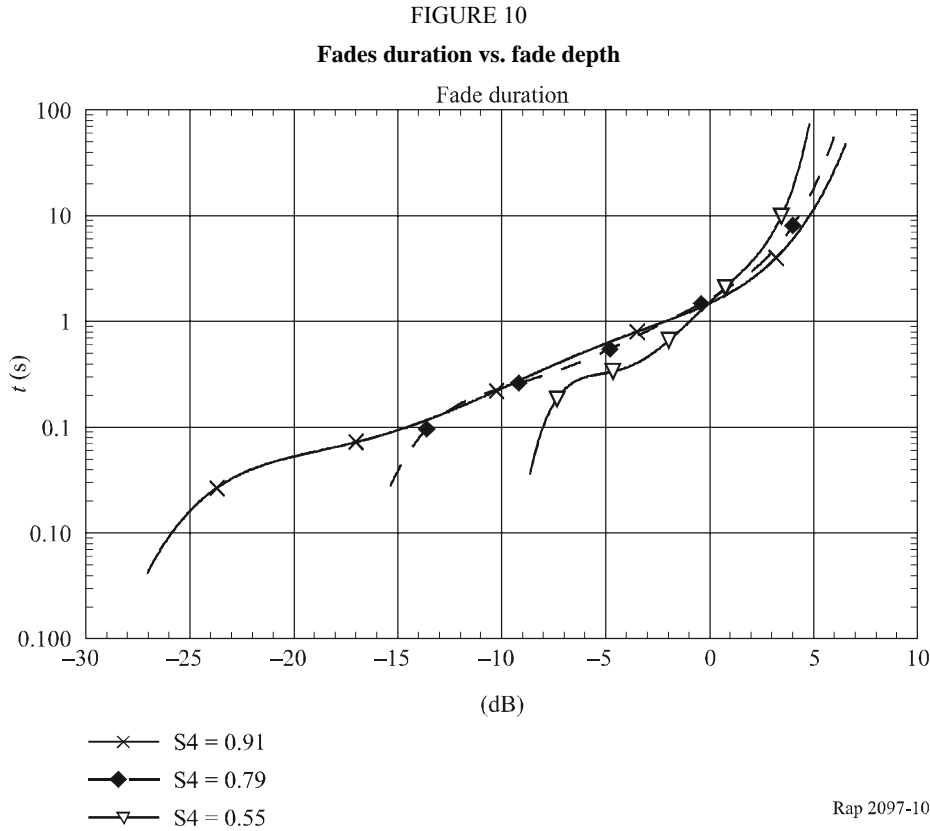


Figure 9 shows a typical signal amplitude under severe scintillation conditions ($S_4 = 0.9$). The corresponding fade duration (Fig. 10) always exceeds the pre-integration duration time. As a consequence it corresponds to a degradation of the SNR at receiver level:

$$C/N = C/N_0 + I_s \quad \text{dB} \tag{13}$$

or, with the fractional form:

$$c/n = c/n_0 * I_s \tag{14}$$

where I_s is the scintillation intensity. Its mean value is 1 and it has a Nakagami distribution characterized by S_4 .

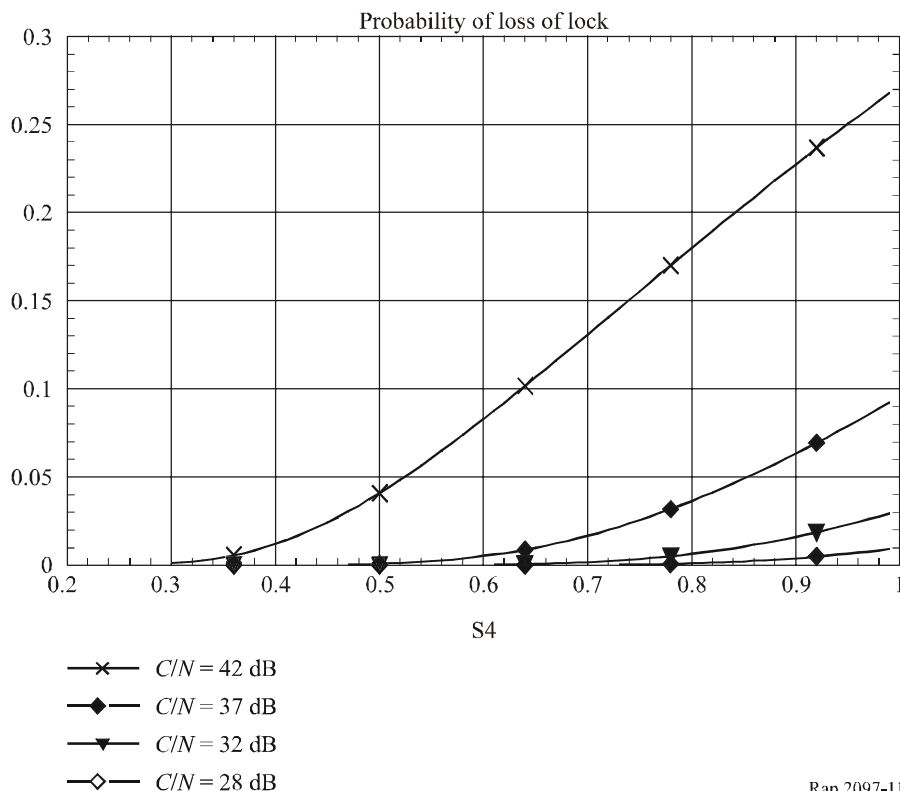
Equation (10) is modified to take the fading into account:

$$\sigma_{\Phi_T}^2 = \frac{B_n}{(c/n_0)I_s} \left[1 + \frac{1}{2\eta(c/n_0)I_s} \right] \tag{15}$$

This relation expresses the thermal noise as a decreasing function of the scintillation intensity. As a result, if σ_{Φ_T} is above the 15° threshold then I_s is below a value computed using equation (15). As I_s distribution is known for a given S_4 , the probability of occurrence of “ $I_s < \text{threshold}$ ” can be evaluated. The result is the probability of loss of lock. Figure 11 presents this probability versus S_4 at given values of the SNR. It can be noticed that links with high SNR are quite robust. On the contrary, links with low values of SNR are likely to be lost.

GISM has an integrated GPS satellite trajectory generator. As an example it has been used to simulate a whole day (24 September 2001) over Naha (Japan, latitude = 26° geographic, 15° magnetic). All visible satellites were used to compute an average probability of loss of lock. The result is 0.21%. In other words, each satellite was 0.21% of the time locked out during that day.

FIGURE 11
Probability of loss of lock vs. S4 for 4 values of the SNR



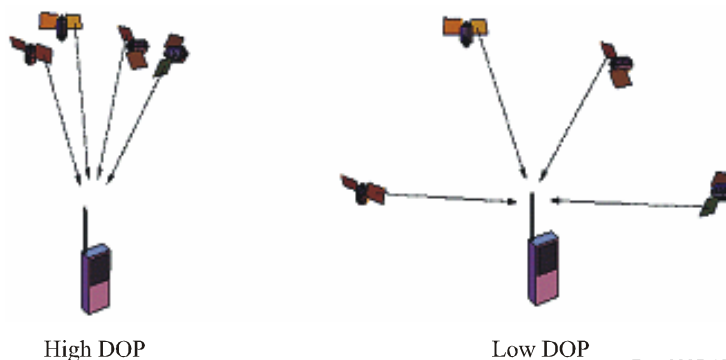
Rap 2097-11

7 Positioning errors

In most cases, scintillations do not affect all visible satellites. If the number of satellites is above 4 then a standard receiver should be able to provide navigation information. However, the number of satellites and their positions affect the positioning precision. The dilution of precision (DOP) is usually used to quantify this precision. The DOP is related to the geometrical distribution of the visible constellation. The scheme on Fig. 12 shows how the DOP is related to the satellites positions. The DOP is used to derive the positioning error, σ_p , from the user equivalent range error (UERE):

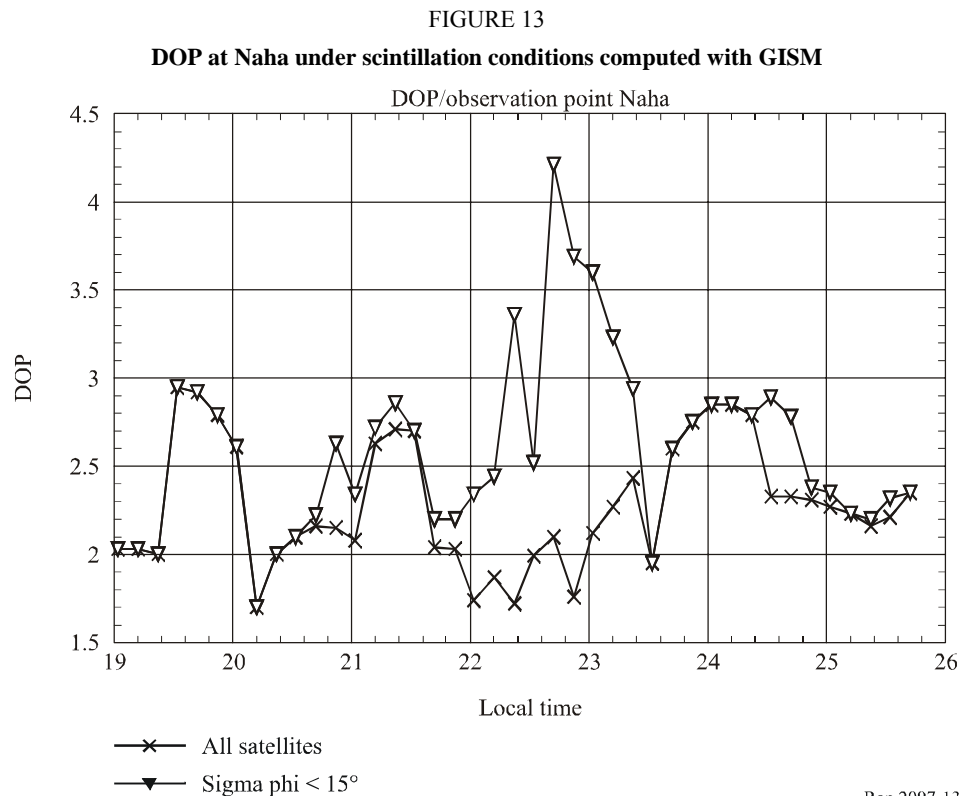
$$\sigma_p = \text{DOP} * \text{UERE} \tag{16}$$

FIGURE 12
DOP and constellation



Rap 2097-12

GISM was used to compute all scintillation parameters for each GPS satellite visible from Naha (Japan). The tracking error was derived from these parameters and from typical receiver characteristics. Satellites with tracking error above the 15° threshold were ignored for the DOP evaluation. Figure 13 presents the resulting DOP, compared with the DOP of the unaffected constellation. In the worst cases, the DOP during scintillation can be twice as high than under normal conditions.

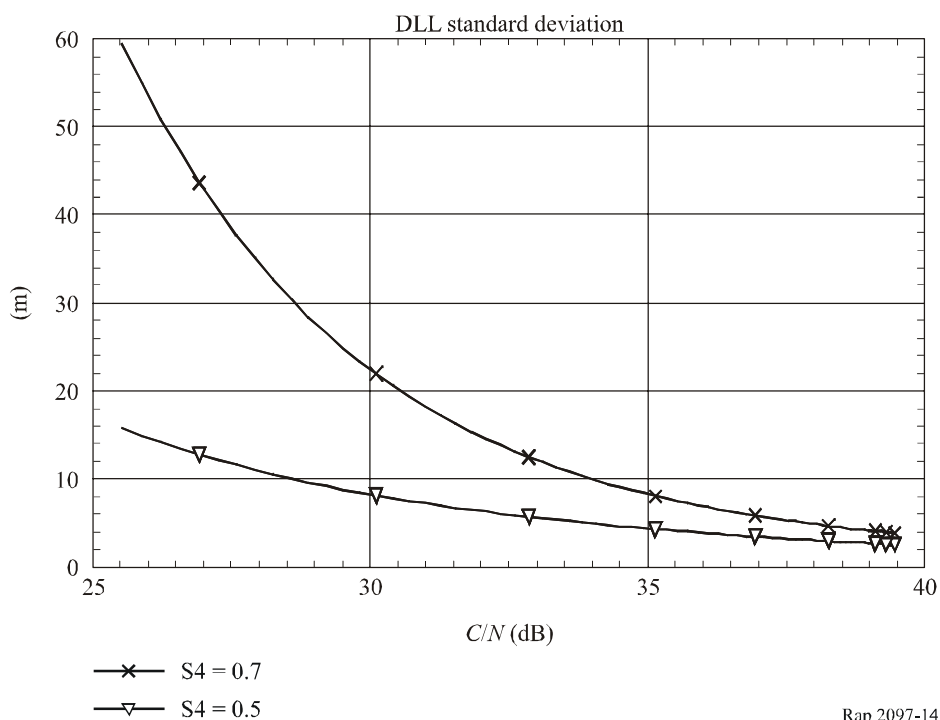


Rap 2097-13

Even if the signal transmitted from a GPS satellite is not lost, it can alter the position accuracy. One of the DLL functions is the measurement of the delay between the code carried by the GPS signal and the receiver internal clock. This delay is an estimation of the time needed by the GPS signal to reach the receiver. The receiver is then able to compute the distance of the satellite. Errors in this estimation are collected in the UERE. To take into account the scintillations, we have to consider the DLL tracking errors.

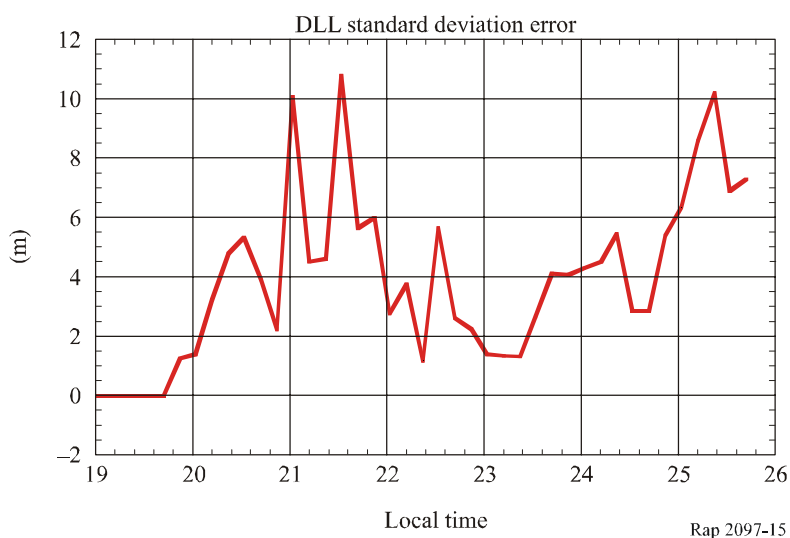
The DLL can be studied like the PLL to evaluate its tracking error variance in degrees. The UERE due to scintillations can then be deduced with a product with the chip length (equal to 293 m for L1 [Ward, 1996]). The results are shown in Fig. 14. These results seem to show high degradation of the UERE. It must be combined with Fig. 8: satellites with high DLL tracking errors have also high PLL tracking errors and therefore they might be considered as lost and do not contribute to the UERE.

FIGURE 14
DLL tracking error vs. C/N_0



The combination of both effects is presented in Fig. 15. Satellites with PLL tracking errors above 15° were considered invisible for the DOP calculation. All other links with visible satellites were used to compute a mean UERE contribution due to scintillation.

FIGURE 15
Positioning error at Naha (Japan) under scintillation conditions, computed with GISM



8 Simultaneous loss of lock

Taking the 15° criteria for loss of lock threshold, the links with such a phase standard deviation level have been selected. This gives the number of satellites simultaneously locked out. The result is reported on Fig. 16. Three satellites may be lost simultaneously in a few cases, which correspond to

the highest values of the DOP. As a comparison, the measurements results are presented on Fig. 17 [Matsunaga, 2002]. Locked-out links are in brown. Strong scintillations are in pink. Quite similar results are obtained. Three satellites are locked out simultaneously in some cases and even four in extreme cases.

FIGURE 16

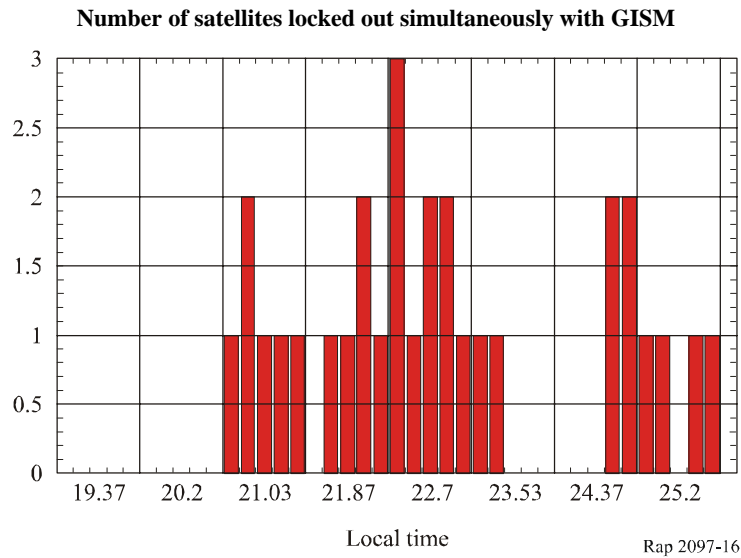
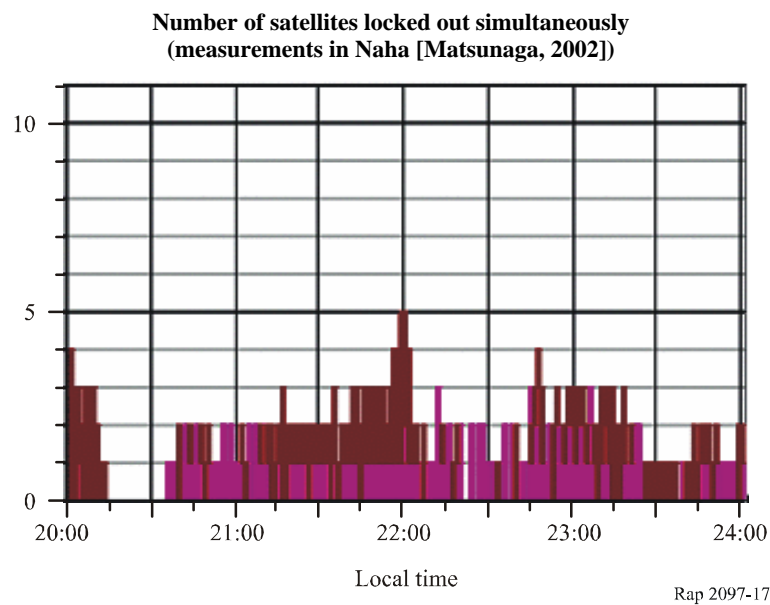


FIGURE 17

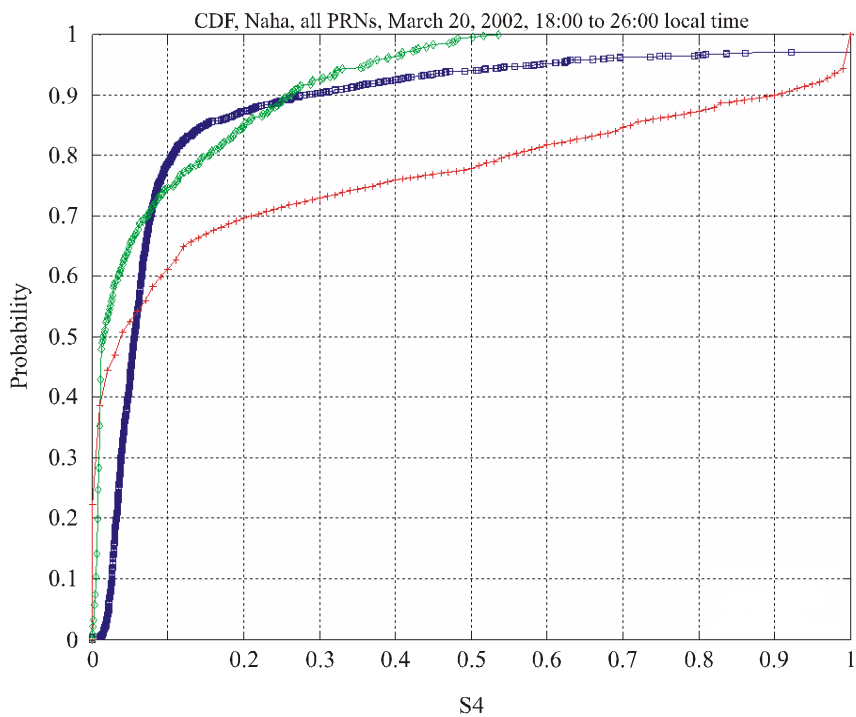
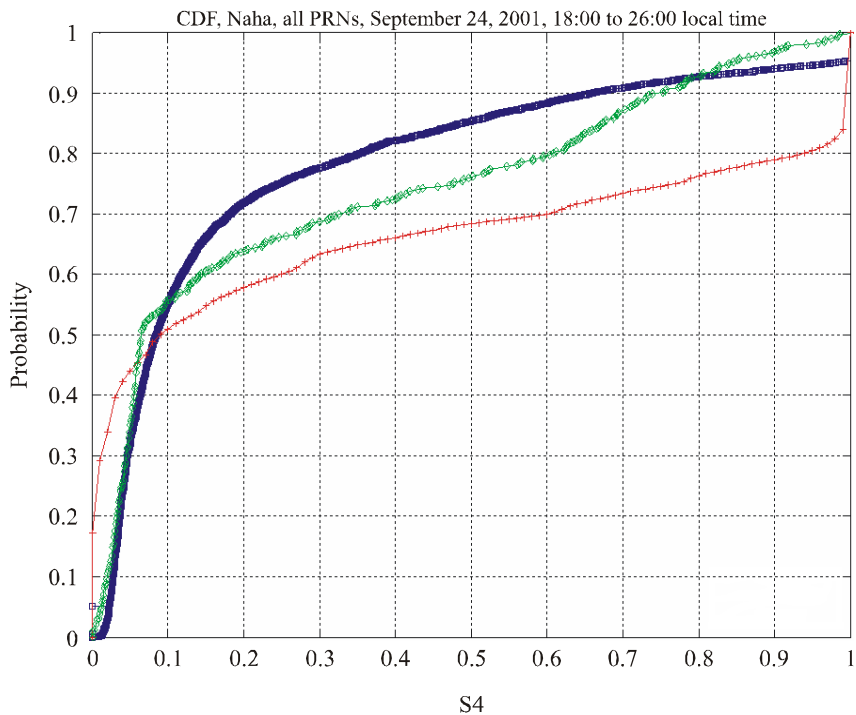


9 Comparisons models results and measurements

The comparisons with GPS links measurements have been done for two days [El Arini *et al.*, 2003] in Naha (Japan), one with a high value of the SSN: 200, and the other with a lower value: 85. All PRNs have been considered. The cumulative probabilities are presented below for these two days. Measurements are in blue and GISM results are in green.

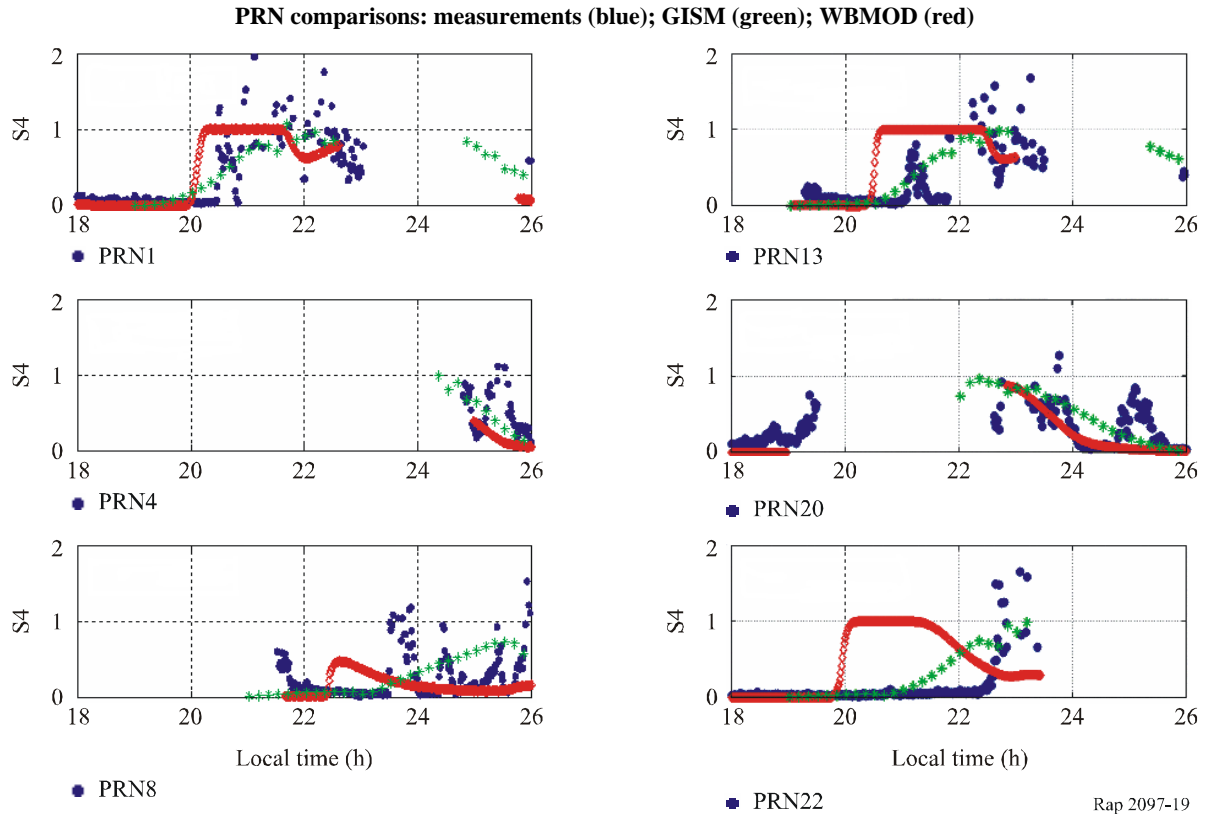
FIGURE 18

Comparison between GISM results and measurements.
 Left curve SSN = 200; right curve SSN = 85



—■— Measured
 —+— WBMOD
 —◇— GISM

FIGURE 19



References

- AARONS, J. [1982] Global morphology of ionospheric scintillations. *Proc. of the IEEE*, 70, 4.
- AFRAIMOVITCH, E.L., ZHERENTSOV G.A. and ZVERZDIN V.N. [1994] Characteristics of small scale irregularities as deduced from scintillation observations of radio signals from satellites ETS-2 and Polar bear at Irkutsk. *Radio Sci.*, Vol. 29, 4.
- BÉNIGUEL, Y. [May-June 2002] Global Ionospheric Propagation Model (GIM): A propagation model for scintillations of transmitted signals. *Radio Sci.*
- CONKER, R.S., EL-ARINI, M.B., HEGARTY, C.J. and HSIAO, T. [January/February 2003] Modeling the effects of ionospheric scintillation on GPS/SBAS Availability. *Radio Sci.*
- DOHERTY, P., DELAY, S. and VALLADARES, C. [2000] Ionospheric scintillations effects in the equatorial and Polar regions. ION GPS Symposium, Salt Lake City, United States of America.
- EL ARINI, M.B., CONKER, R., BÉNIGUEL, Y. and ADAM, J-P [September 2003] Comparing measured S4 with the calculated S4 by the WBMOD and GISM at Naha, Japan. Private communication.
- MATSUNAGA, K. [2002] Observation of ionospheric scintillations on GPS signals in Japan. ION Symposium.
- Mc DOUGALL, J.W. [1981] Distributions of the irregularities which produce ionospheric scintillations. *Atmospheric and terrestrial physics*. Vol. 43.
- WARD, P. [1996] *Satellite signal acquisition and tracking. Understanding GPS Principles and Applications*, Ed. E.D. Kaplan, Artech House, Boston, United States of America, p. 119-208.